Post-test results of the QUENCH-16 bundle test on air ingress: complex cladding oxidation during reflood and combined hydrogen

J. Stuckert, M. Steinbrück

QWS18, Karlsruhe 2012

Institute for Applied Materials; Program NUKLEAR

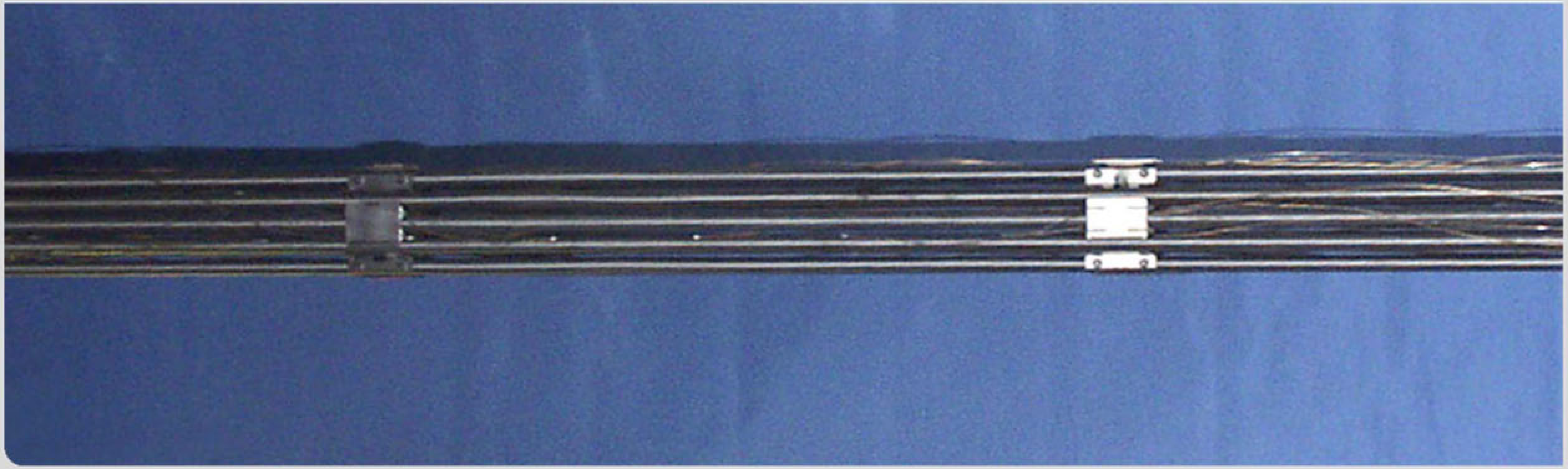

Previous bundle air ingress experiments

- **CODEX AIT-1, AIT-2 (Zry-4) performed 1999 at AEKI/Budapest: *small bundles with 9 rods***

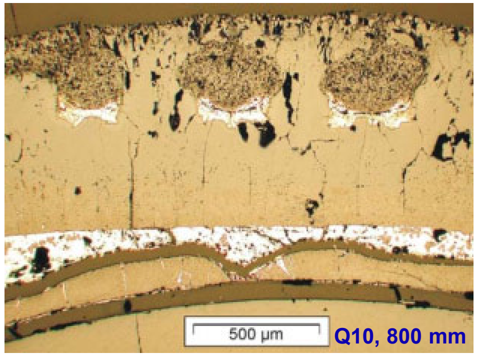

- **QUENCH-10 (Zry-4 claddings) performed 2004 at KIT/Karlsruhe: *strong pre-oxidised bundle***

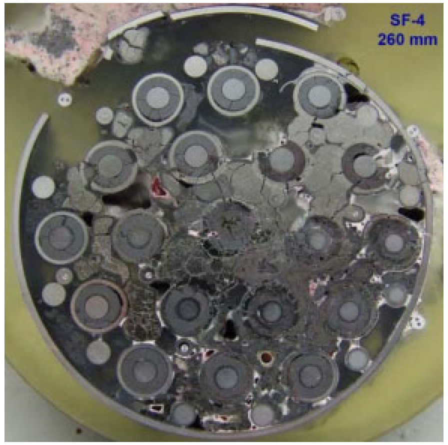

- **PARAMETER-SF4 (E110 claddings) performed 2009 at LUCH/Podolsk*: very high temperatures on reflood initiation with following escalation (bundle melting)***

Objectives of the QUENCH-16 test

- air oxidation after rather moderate pre-oxidation in steam;

- slow oxidation and nitriding of zirconium in high temperature air and transition to rapid oxidation and temperature excursion;

- role of nitrogen under oxygen-starved conditions;

- formation of oxide and nitride layers on the surface of Zr;

- release of hydrogen from oxidised zirconium during air ingress scenario;

- reflooding of oxidised and nitrided bundle by water initiated at temperatures well below the melting point of the cladding, release of nitrogen.

QUENCH facility

QUENCH-16 facility features:

1) <u>controllable synthetic air input</u>;

2) Krypton filling of rods;

3) temperature control for off-gas pipe (to avoid the steam condensation)

4) control of pressure in space between shroud and jacket

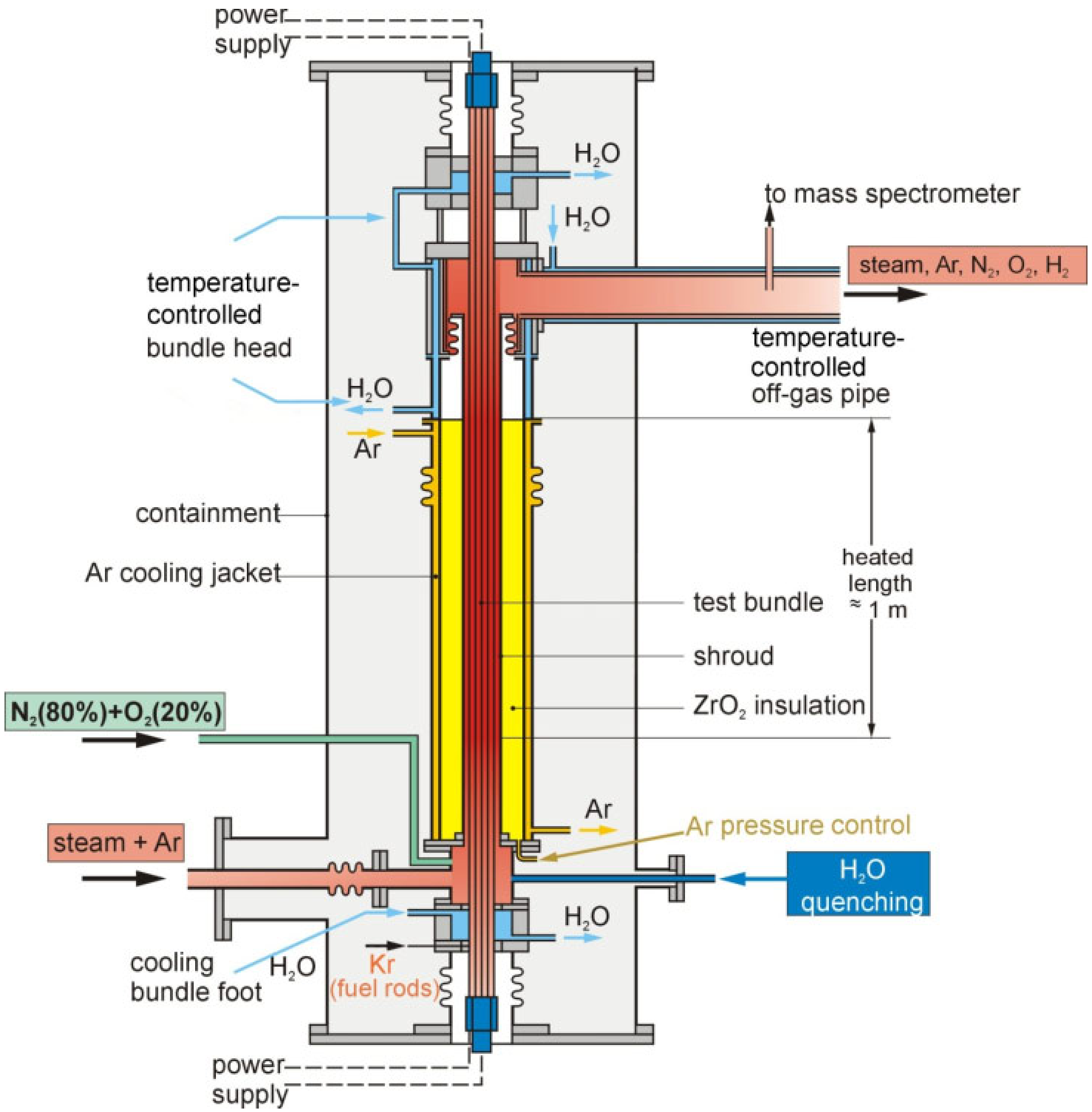

Cross section of the PWR test column

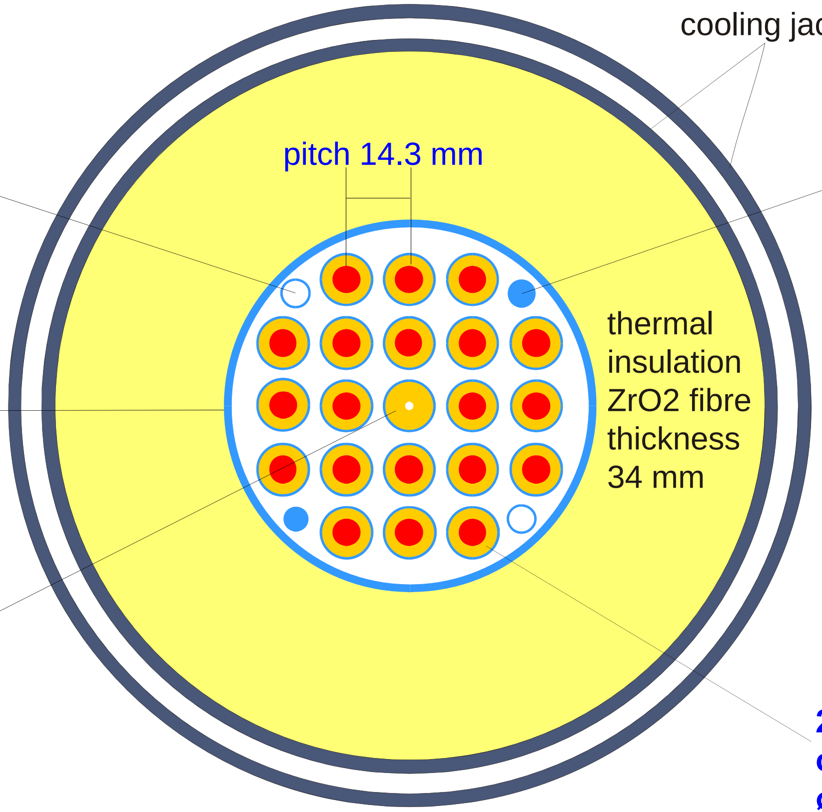

cooling jacket

2 removable
corner rods
Zry-4 ø6 mm

2 instrumented tubes
Zry-4 ø6/4.2 mm

pitch 14.3 mm

thermal
insulation
ZrO2 fibre
thickness
34 mm

shroud Zry-4
ø88.9/82.8mm

1 unheated rod
cladding Zry-4
ø10.75/9.3 mm
central thermocouple
pellet ZrO_2
ø9.15/2.5mm

20 heated rods
cladding Zry-4
ø10.75/9.3 mm
W-heater
ø6mm
pellet ZrO_2
ø9.15/6.15mm

QUENCH-16 test progression

test performed on 27.07.2011 at KIT/IAM
according to pre-test calculations from PSI, GRS, EdF

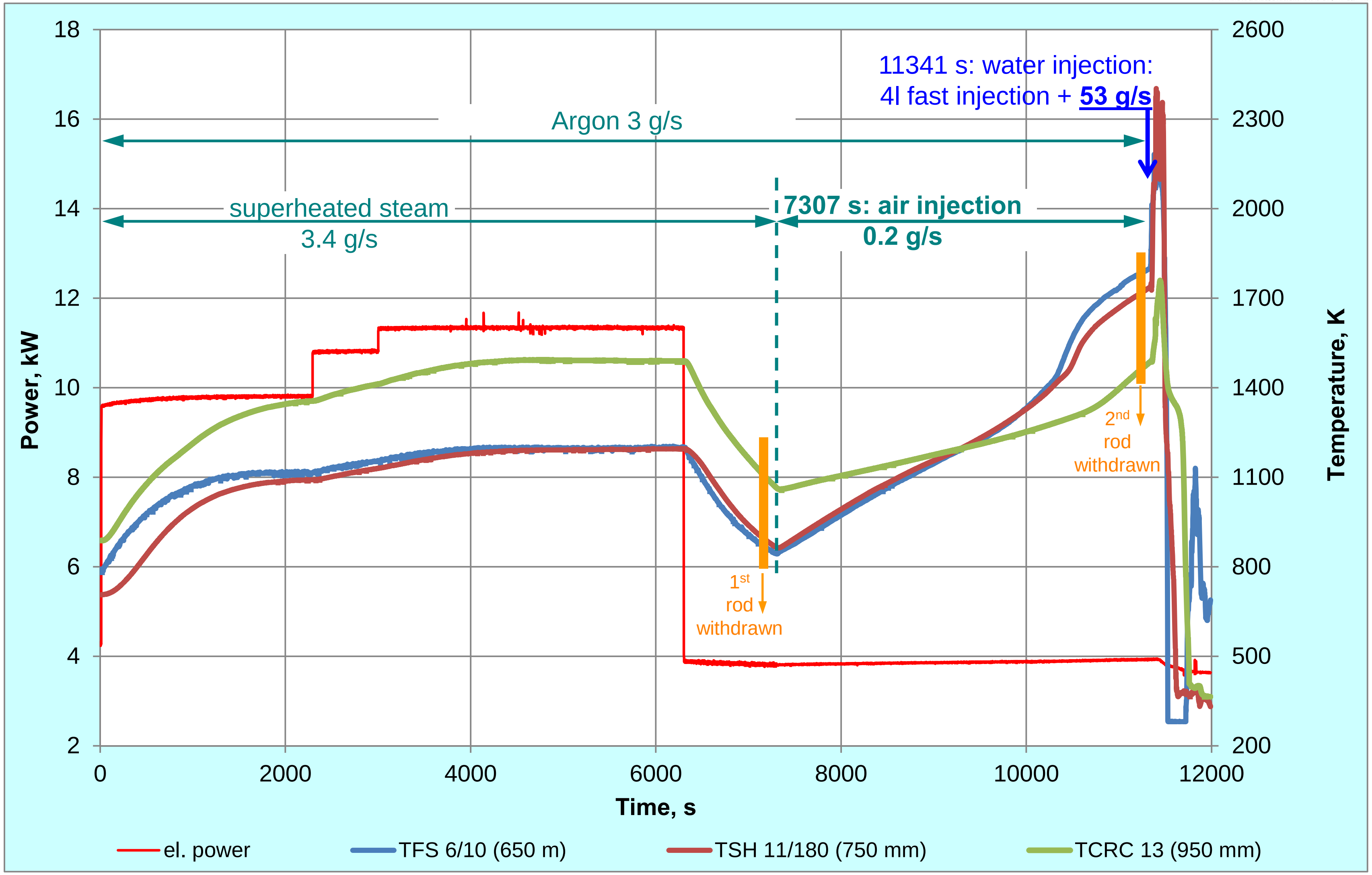

Axial temperature distributions for different test phases

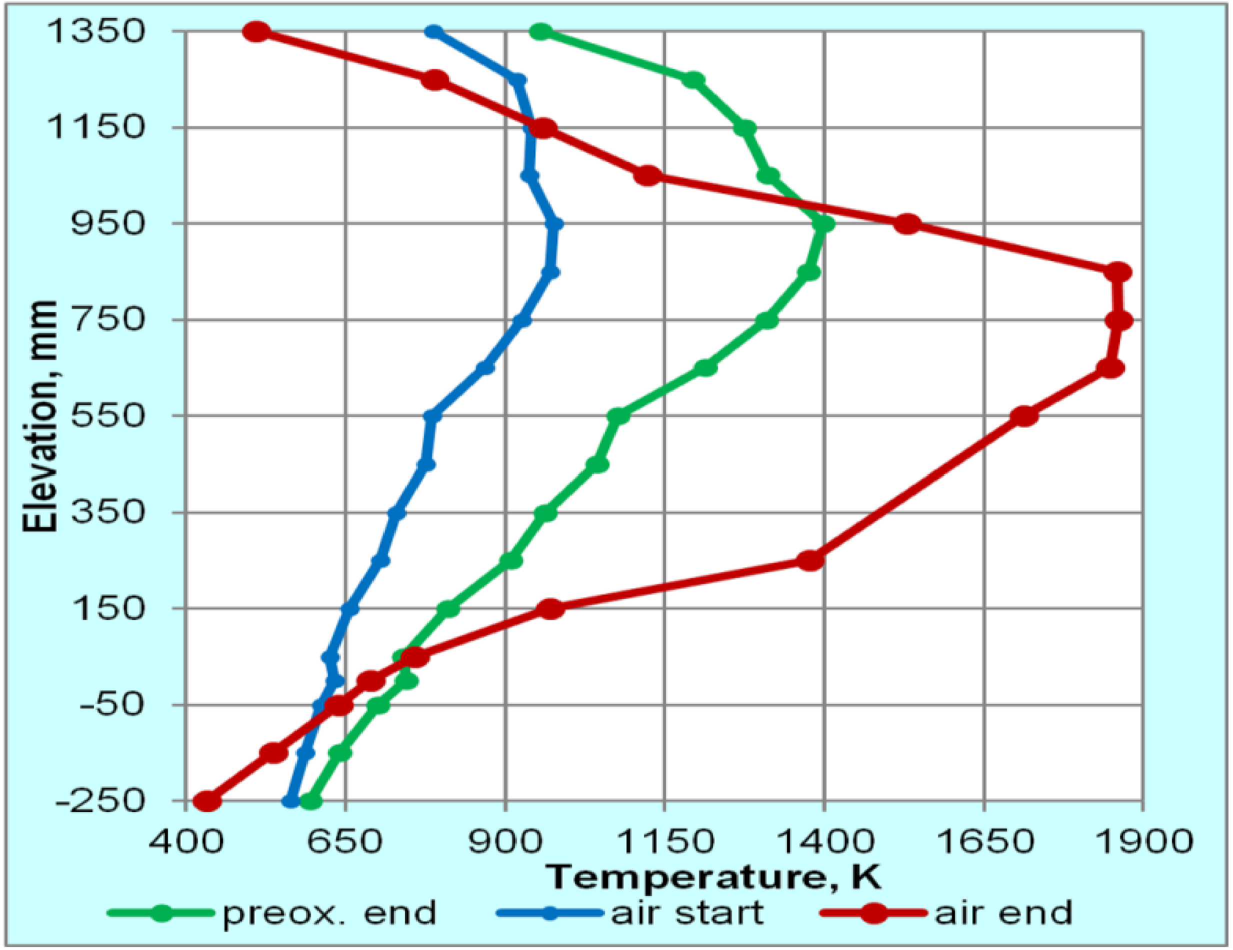

strong growth of temperatures at elevations 250 – 950 mm during the air ingress phase

Consumption of nitrogen and oxygen during air ingress phase:
data of mass spectrometer

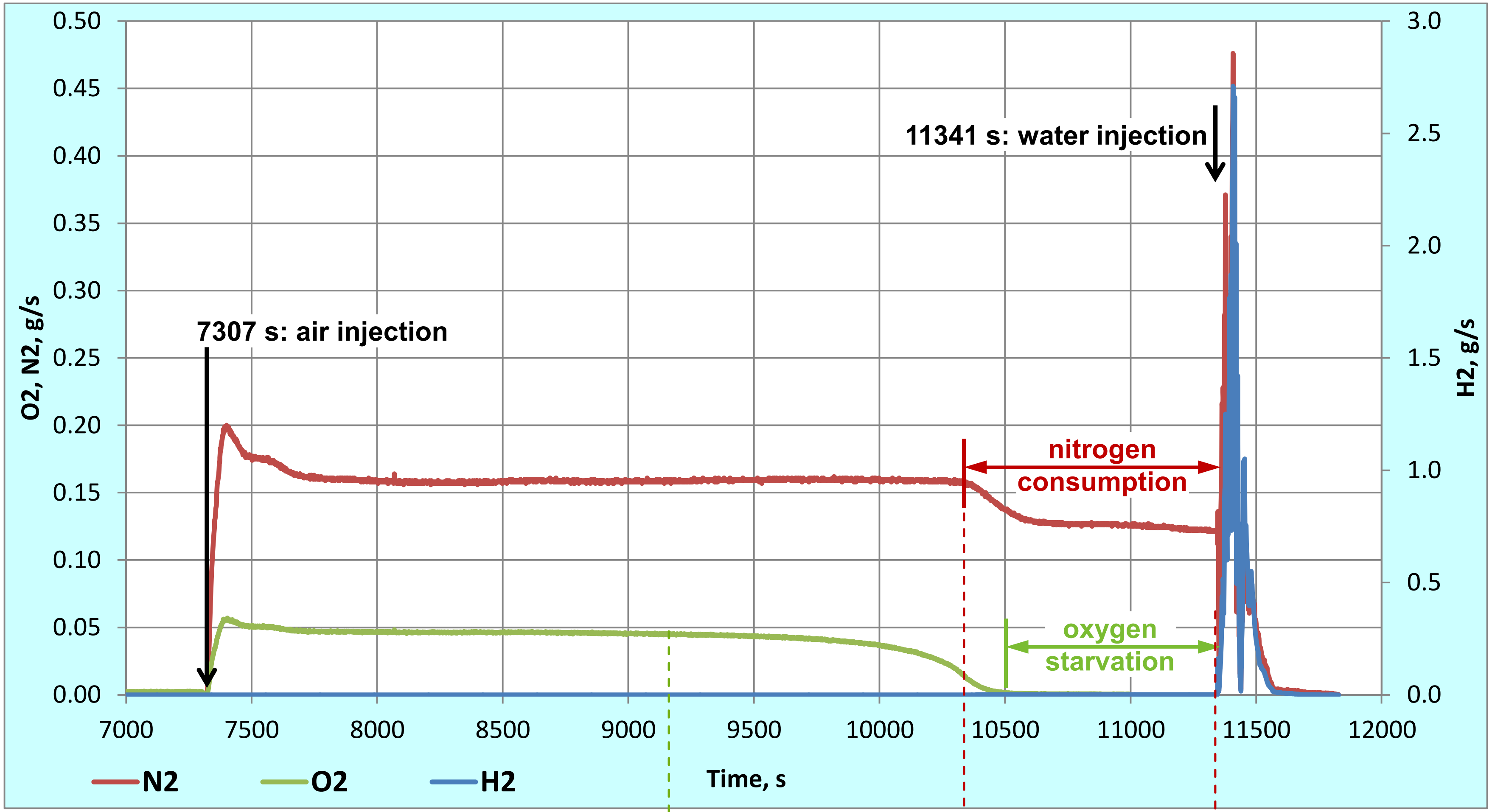

nitrogen uptake: 29 g

oxygen uptake: 58 g

Corner rod D withdrawn from the bundle on the end of the air ingress phase: nitride formation between 300 and 900 mm

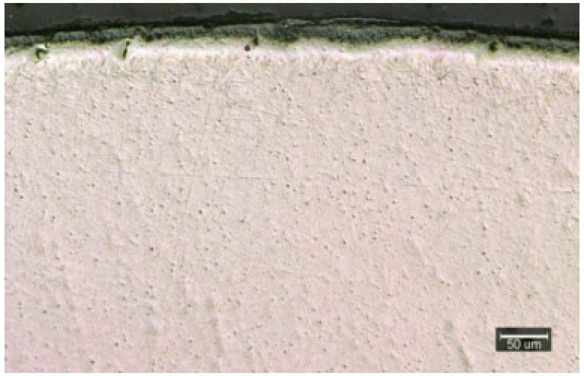	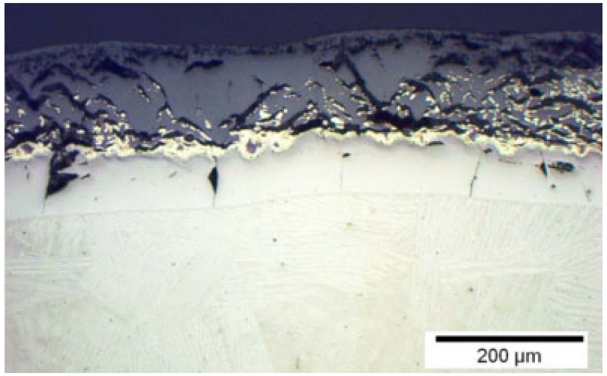	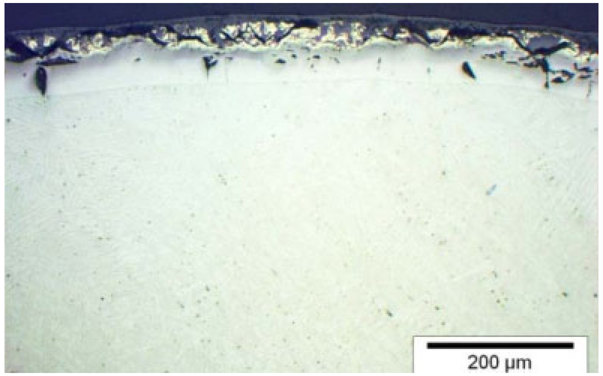
250 mm (1070°C): no nitrides	450 mm (1530°C): strong corrosion; nitrides	650 mm (1400°C): moderate corrosion; nitrides
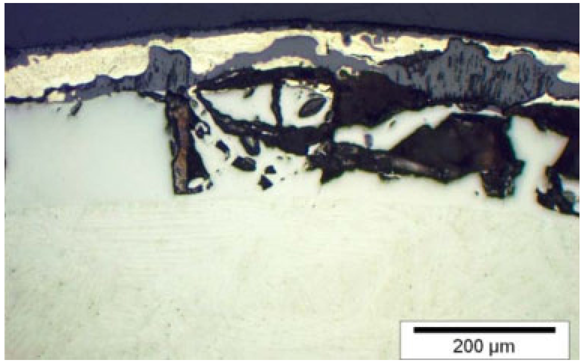	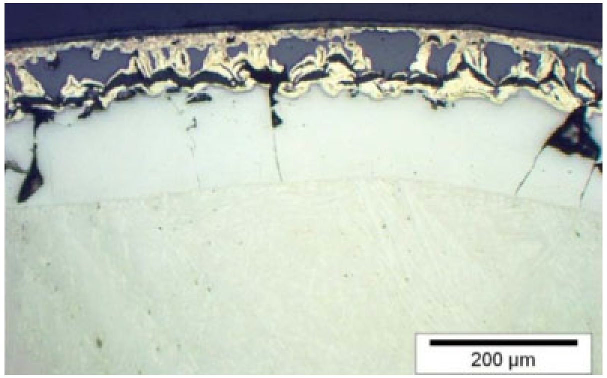	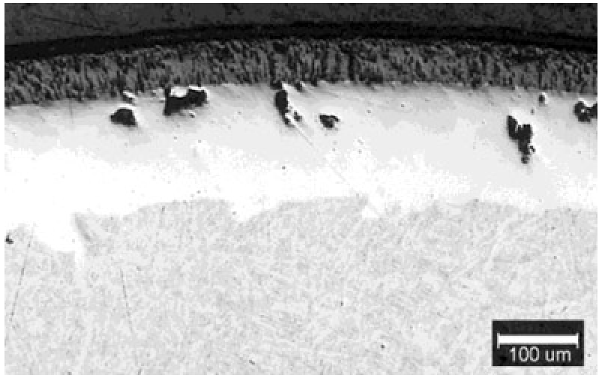
750 mm (1460°C): strong corrosion; nitrides	850 mm (1570°C): strong corrosion; nitrides	950 mm: no nitrides

Temperature escalation (above Zr melting point) and cooldown during reflood

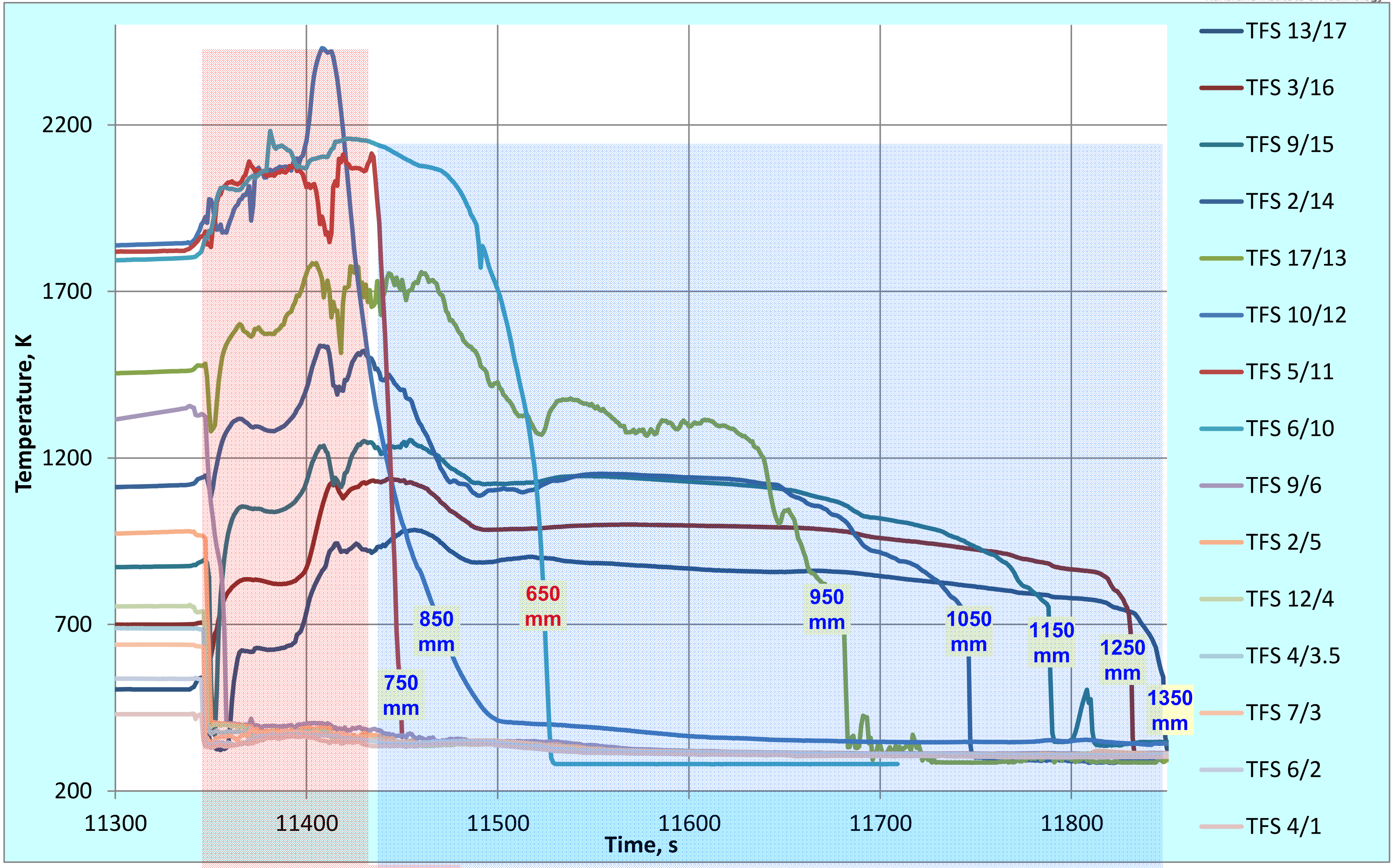

Durations: escalation 100 s cooldown 400 s

Post-test visual investigations by endoscope introduced at the position of the corner rod B: side view

		
350 mm: frozen metallic melt relocated from upper elevations	**420 mm: oxide shells of melt droplets and rivulets**	**600 mm: intensive cladding damaging**
	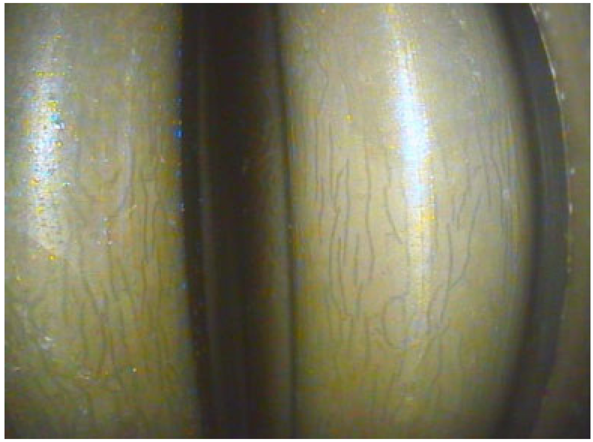	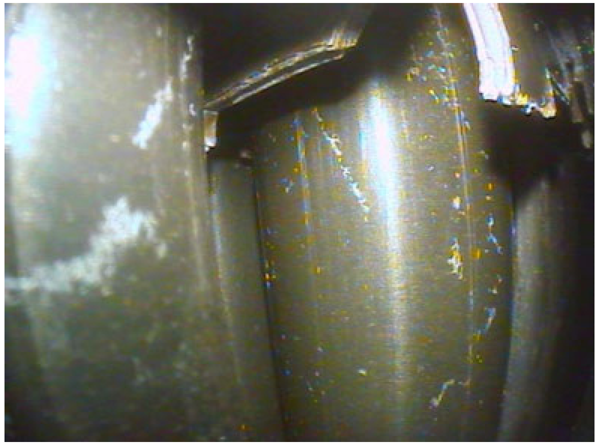
835 mm: spalling of outer scale of oxide layer	**880 mm: not damaged outer scale of oxide layer**	**1050 mm: dark oxide of claddings, intact Grid Spacer #4**

Release of hydrogen and nitrogen during quench phase
/data of mass spectrometer/

hydrogen release: 128 g. 3 main sources: 1) re-oxidation of Zr-nitrides; 2) secondary oxidation of cladding; 3) melt oxidation

nitrogen release during re-oxidation of nitrides: 24 g (from consumed 29 g) -> correspond **7 g hydrogen**

Nitride re-oxidation during quench at elevation 350 mm

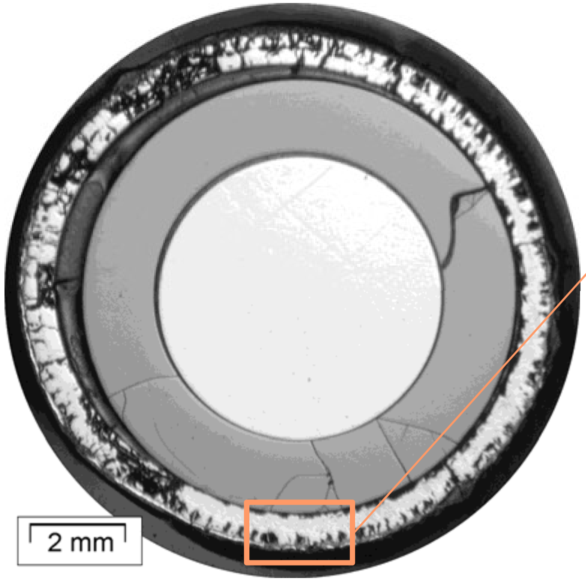

rod #5

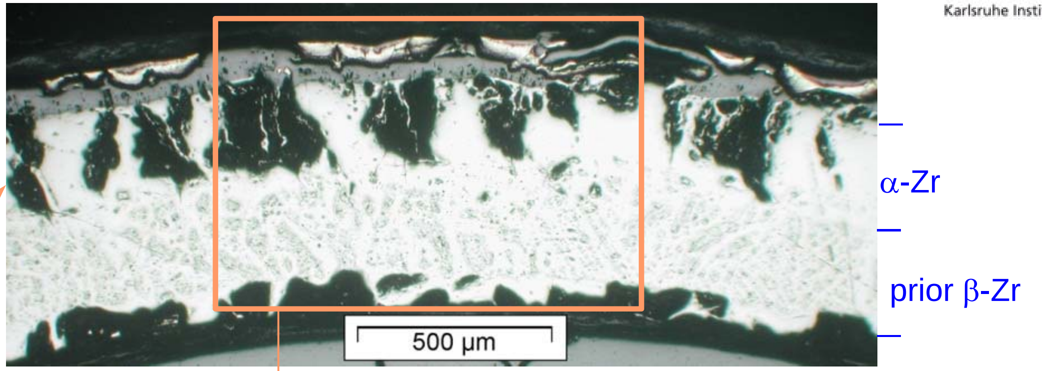

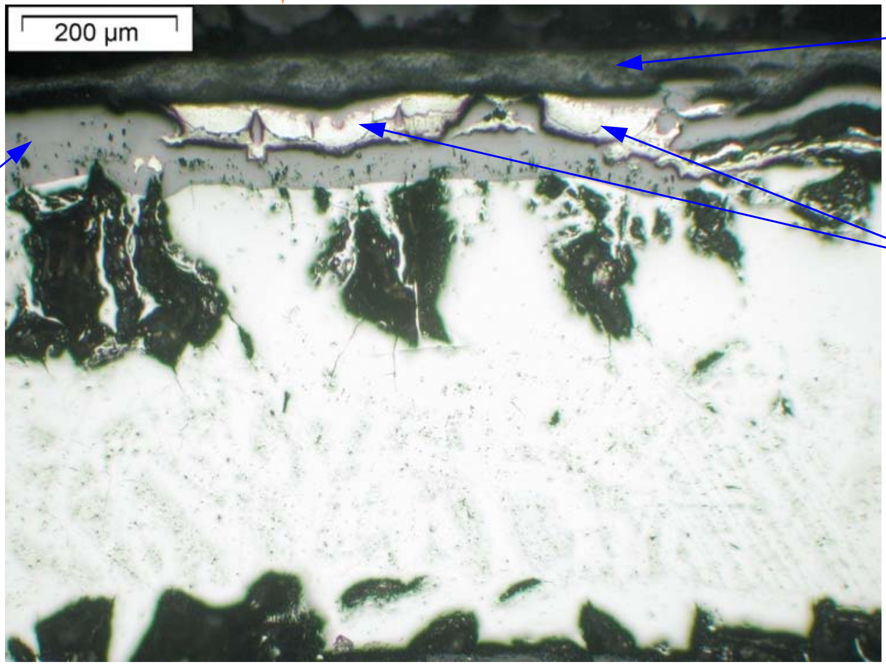

porous oxide scale (re-oxidised during quench)

Zr-nitrides

dense inner oxide (grown during quench phase)

Nitride re-oxidation and secondary cladding oxidation during quench at elevation 450 mm

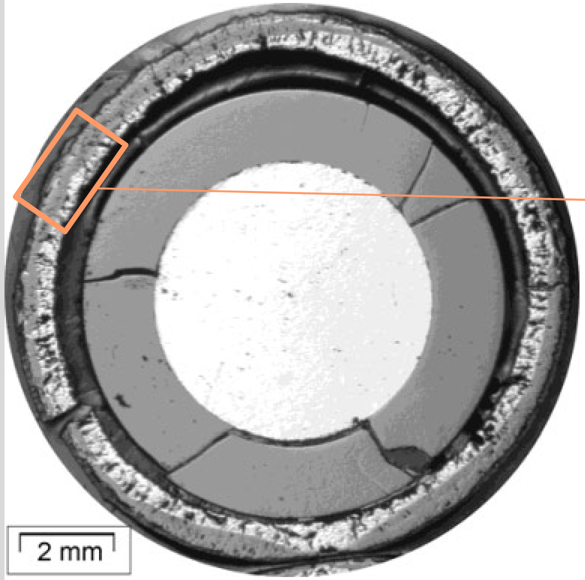

rod #4

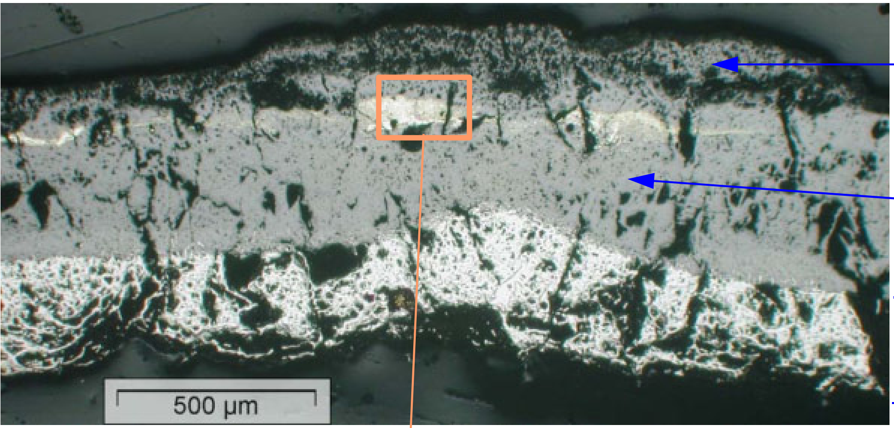

porous oxide scale (re-oxidised during quench)

secondary dense inner oxide (grown during quench phase)

α-Zr(O)

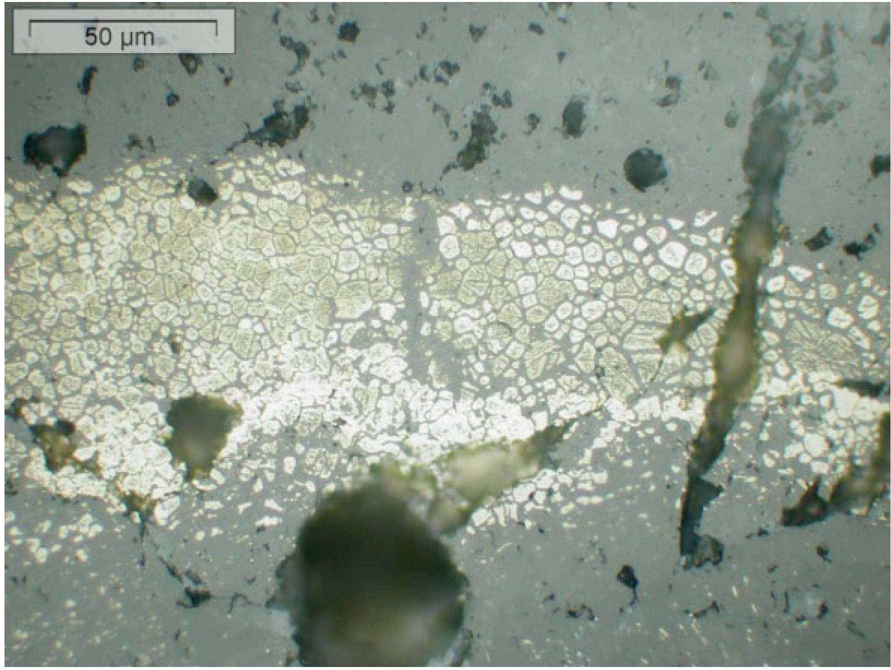

residual Zr-nitrides

Secondary oxidation and melting at elevation 550 mm

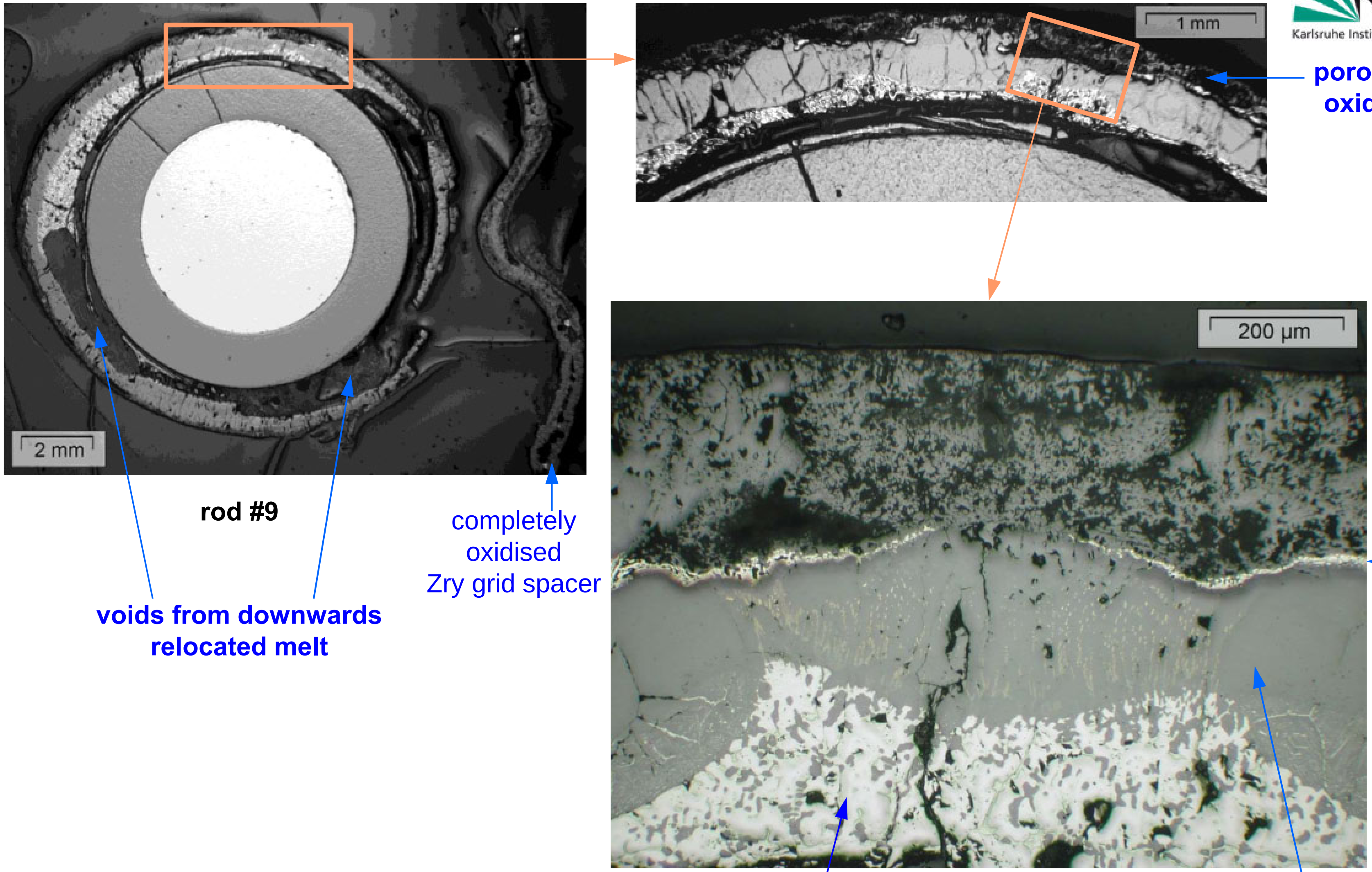

porous outer oxide scale

rod #9

completely oxidised Zry grid spacer

voids from downwards relocated melt

Zr-nitrides

frozen partially oxidised melt

secondary dense inner oxide (grown during quench phase)

Intensive metal formation at elevation 650 mm

rod #9

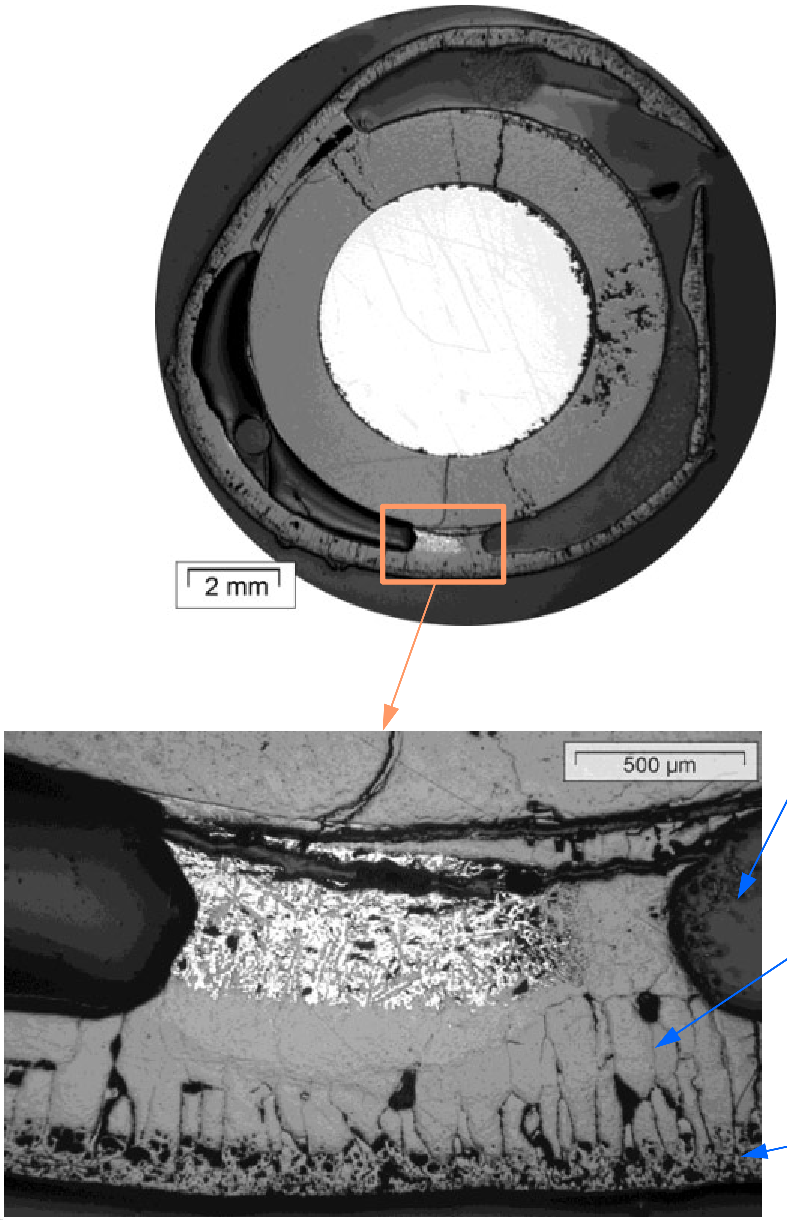

rod #21

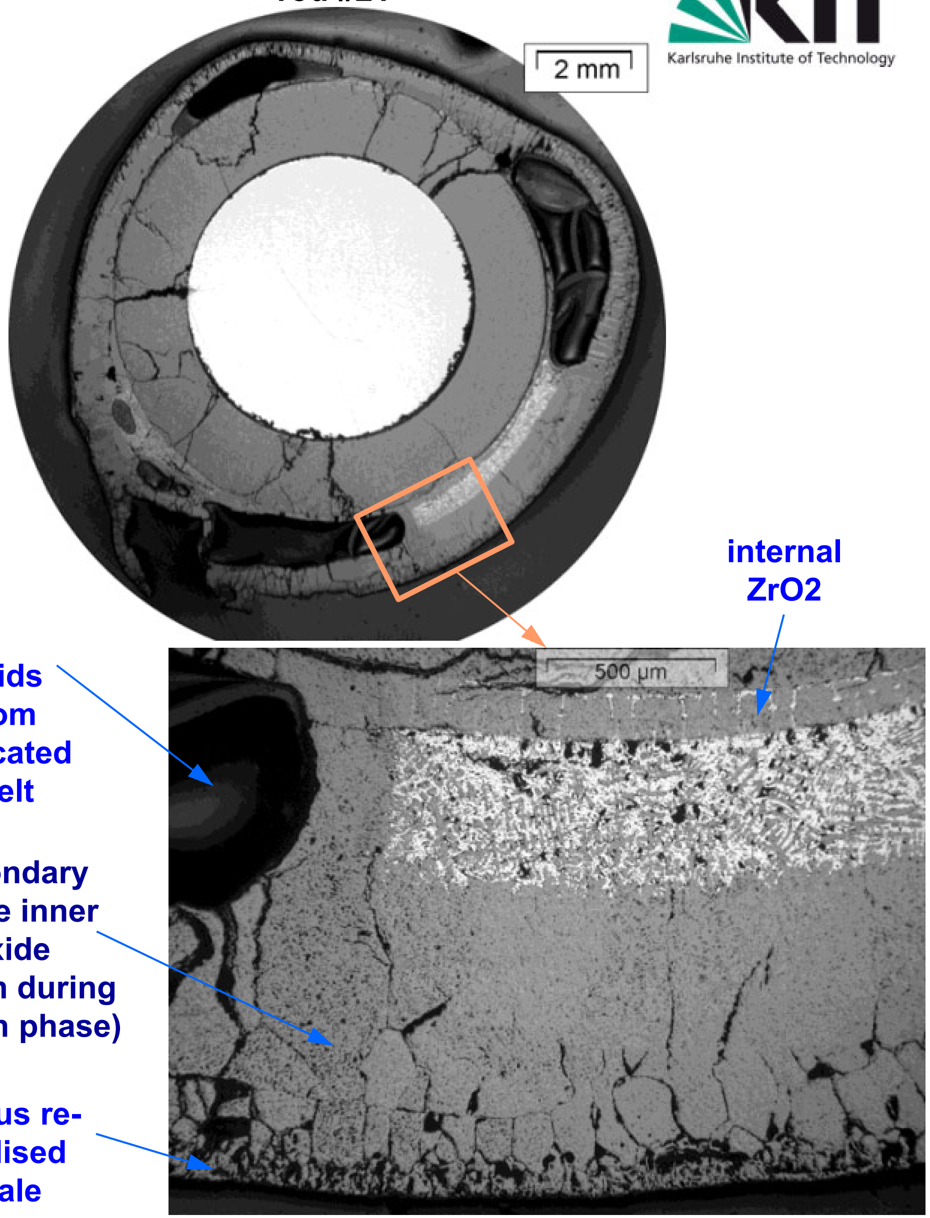

voids from relocated melt

secondary dense inner oxide (grown during quench phase)

porous re-oxidised scale

internal ZrO2

Spalling of re-oxidised scales from secondary oxide at 750 mm

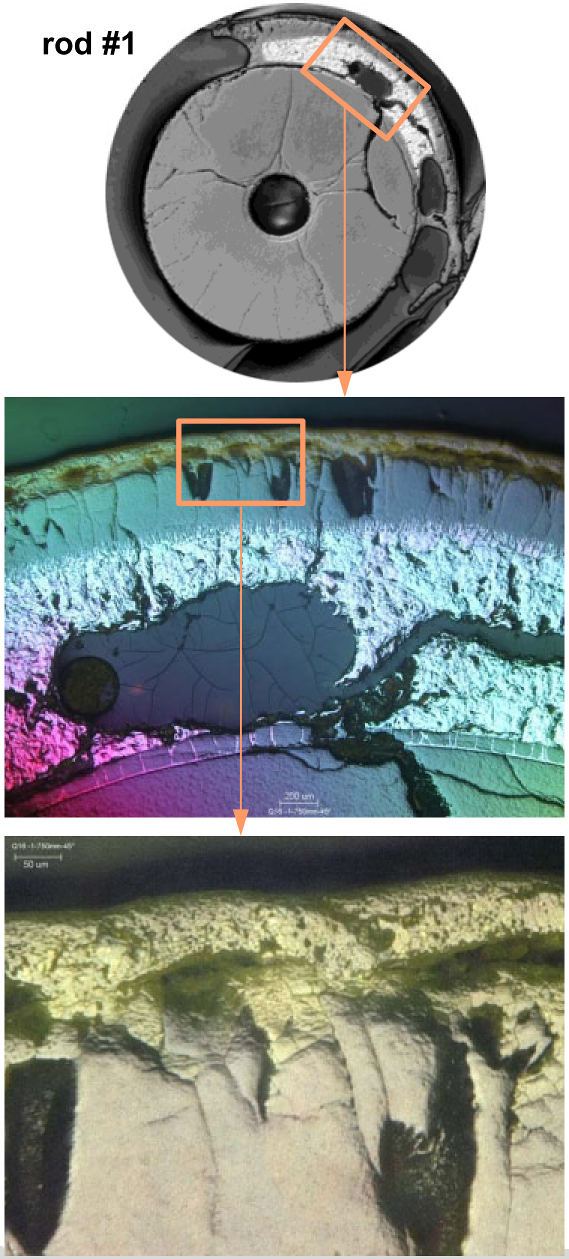

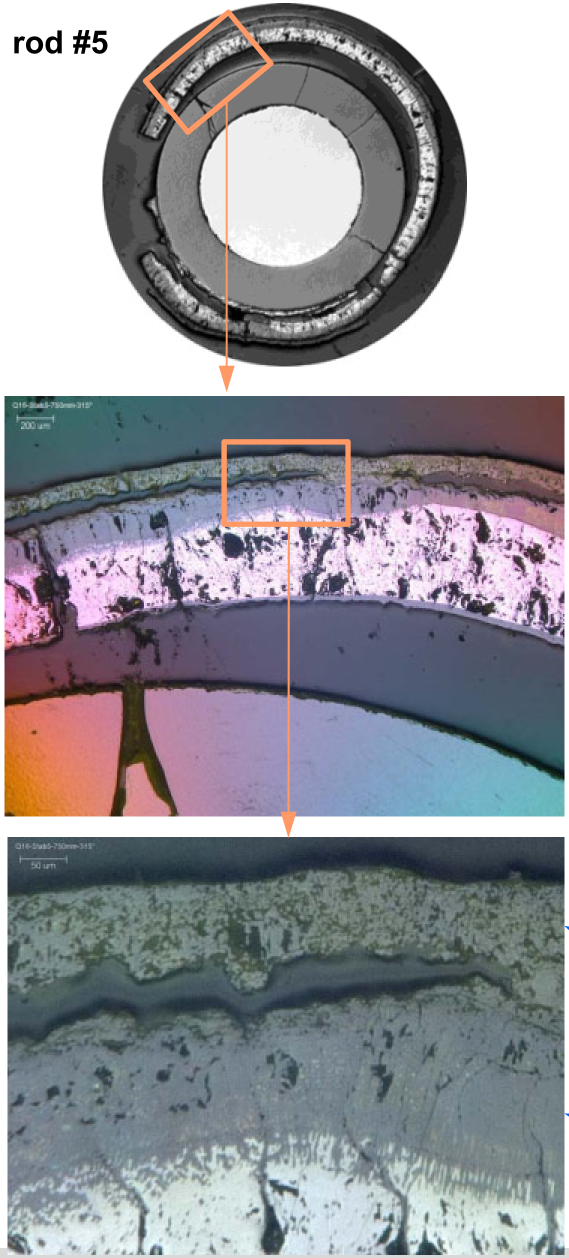

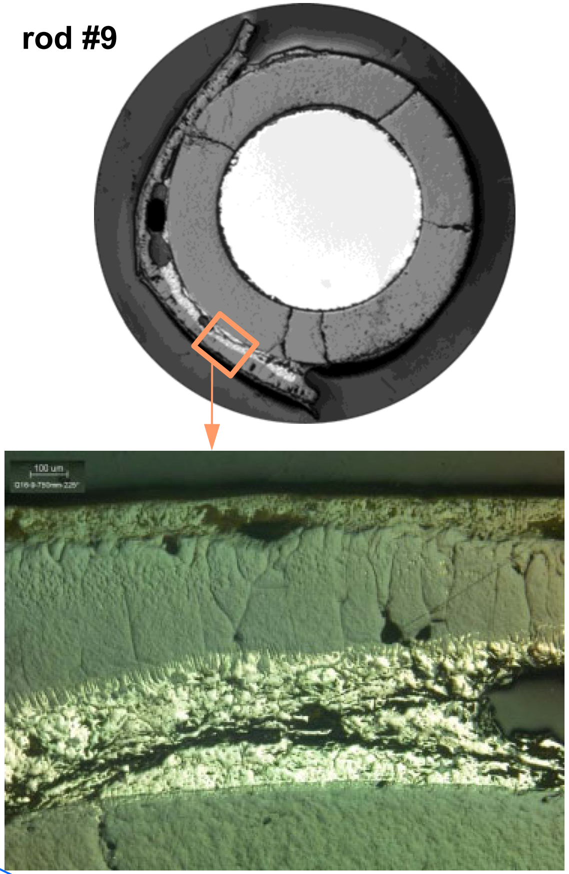

prior nitrided scale re-oxidised during quench and spalled from innner ZrO2 layer growing during quench

Re-oxidation of nitrided scales and metal melting at elevation 850 mm

rod #6

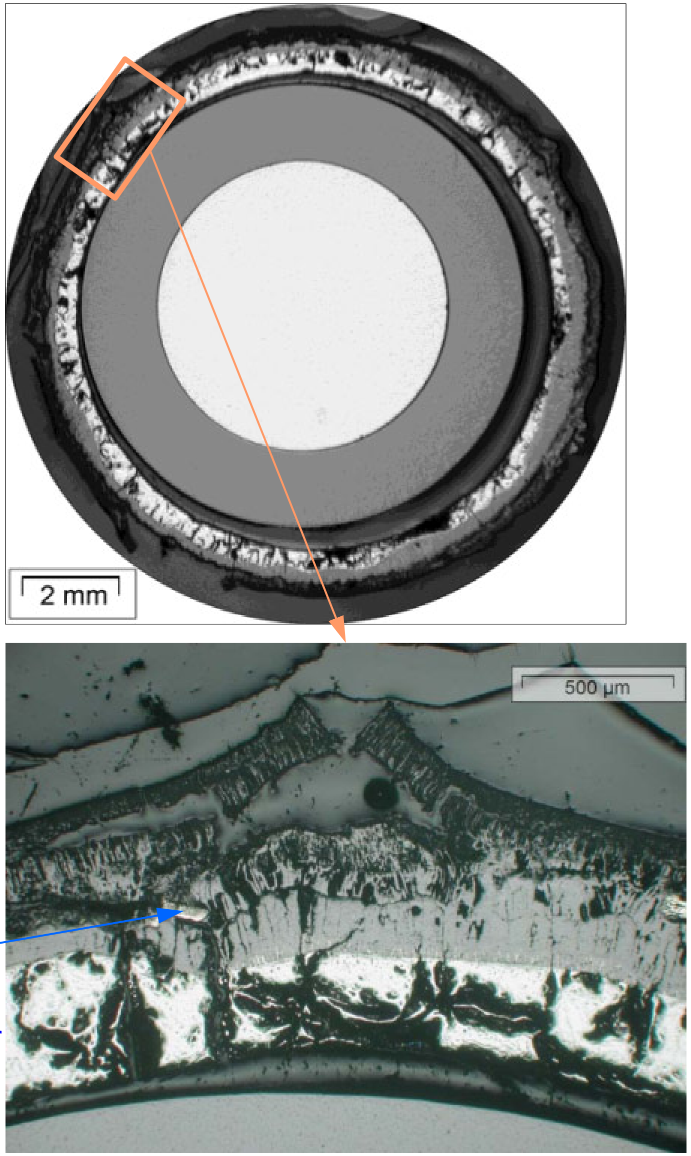

Zr-nitrides

α-Zr

rod #18

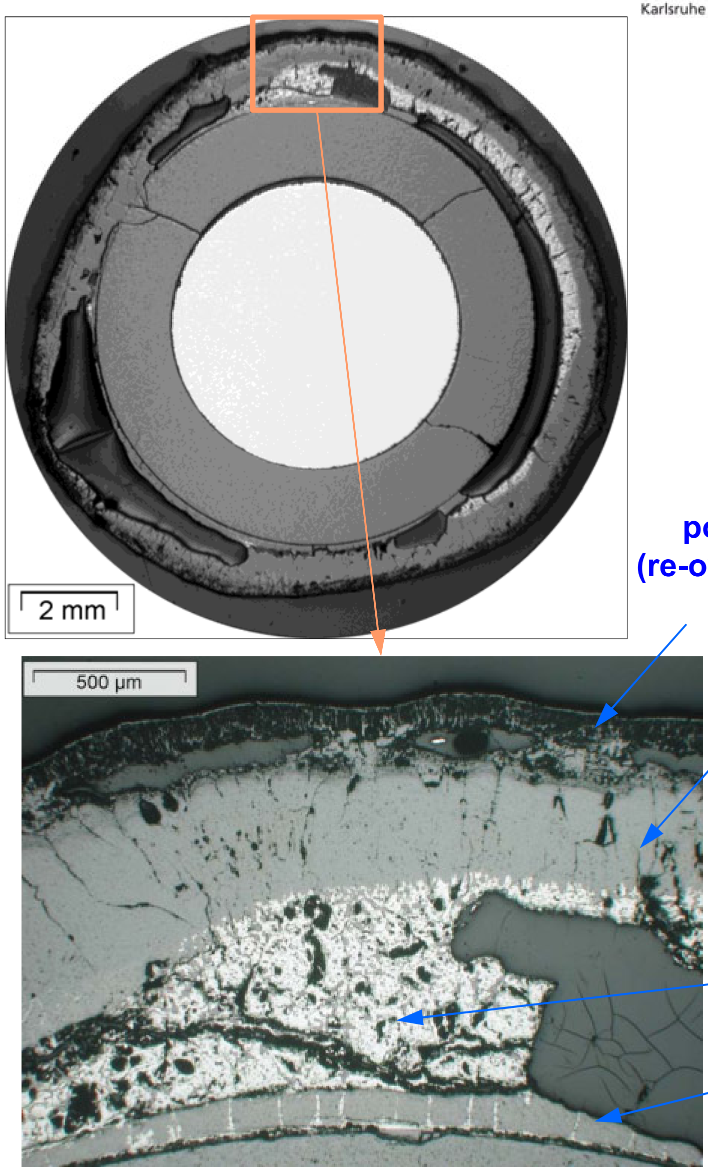

porous scale (re-oxidised during quench)

secondary dense inner oxide (grown during quench phase)

frozen partially oxidised melt

internal oxide layer

Elevation 950 mm: no nitrides, no melt formation

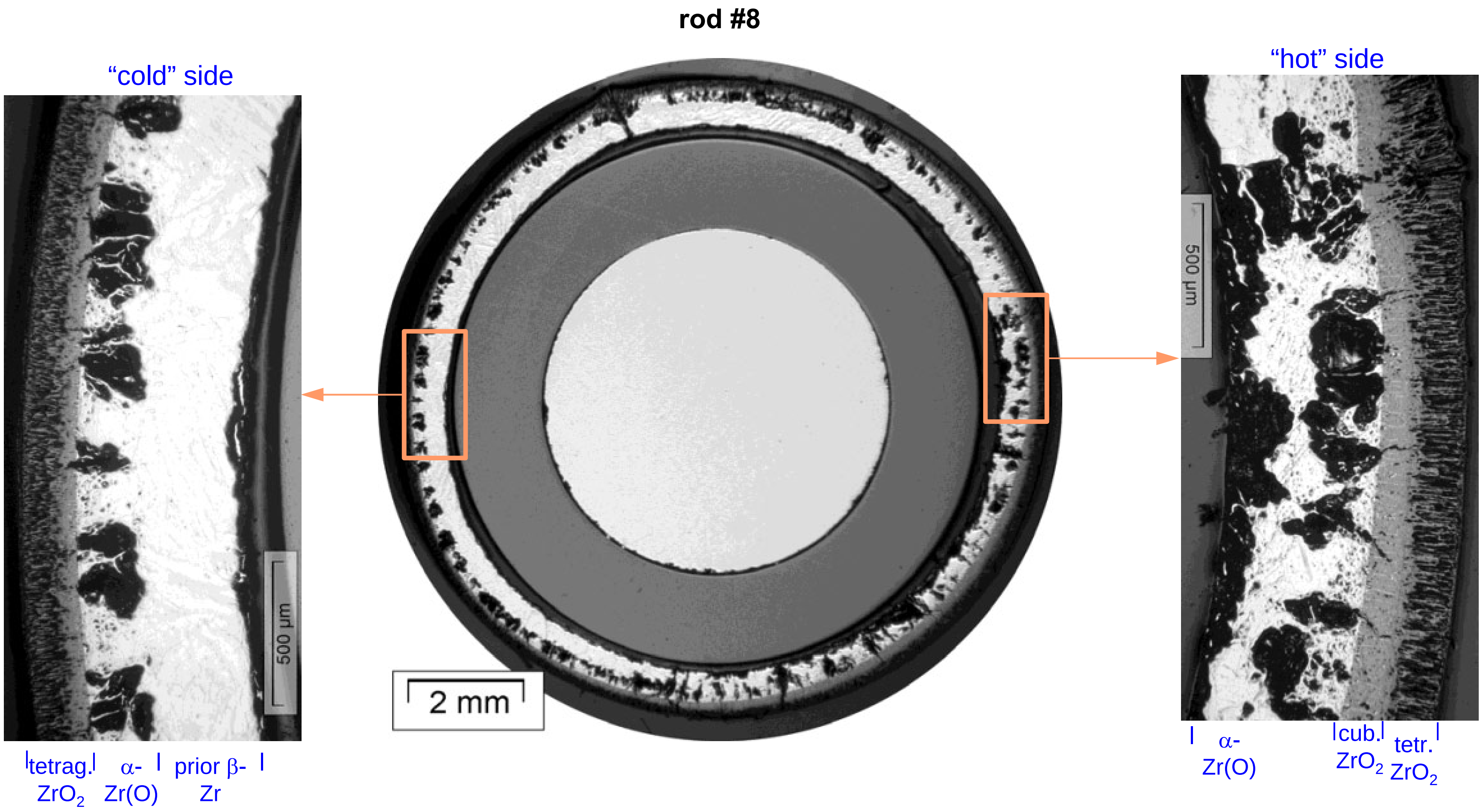

Relative thick oxide layer after pre-oxidation (~100 µm) and low temperatures during air ingress (<1500 K) prevented nitride formation at this elevation

Axial distribution of cladding oxidation rate

850 mm

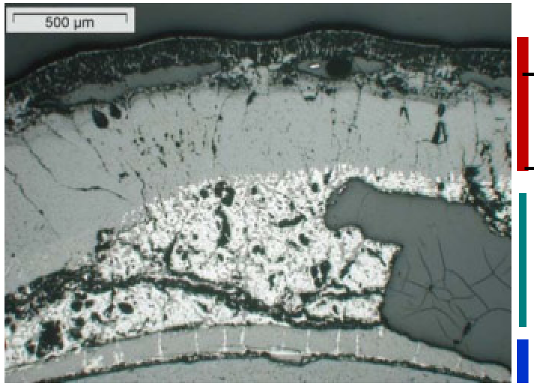

secondary oxide (80% of ZrO2)

550 mm

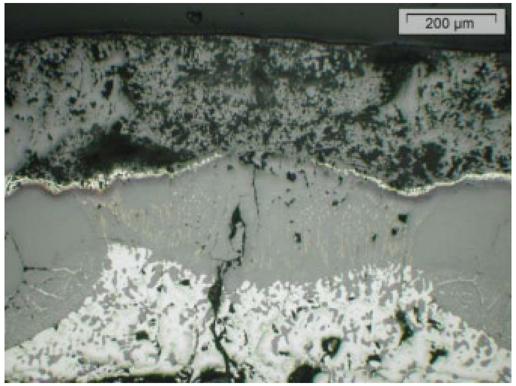

350 mm

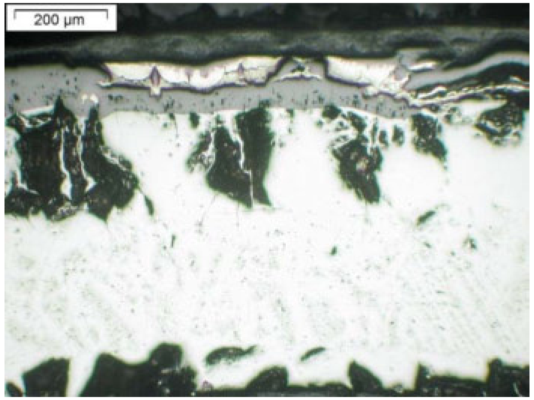

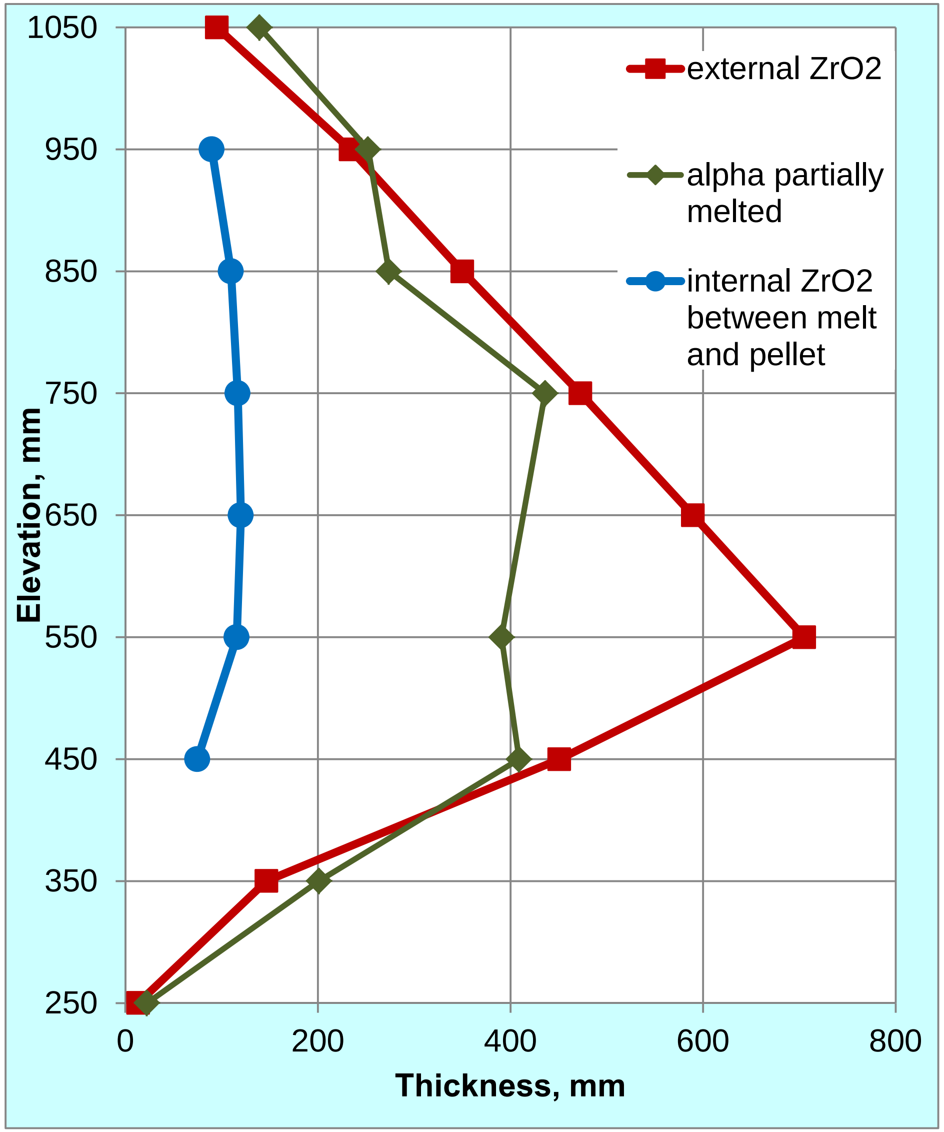

Bundle cross sections: melt formation and relocation

		
350 mm: metallic and oxidised **melt pools**	450 mm: mostly oxidised **melt pools**	550 mm: downwards **relocated cladding metal**
		
650 mm: downwards **relocated cladding metal**	750 mm: downwards **relocated cladding metal**	850 mm: outer oxide layer not failed

Frozen melt at elevation 350 mm: not oxidised and oxidised melt

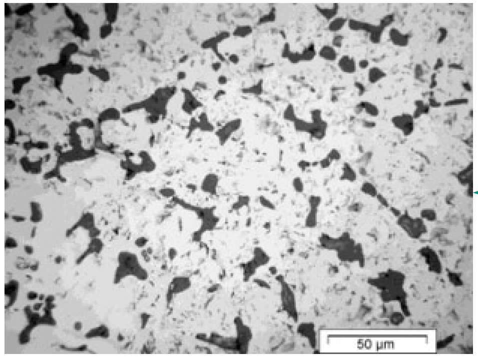

grey porous region;
precipitates 10%

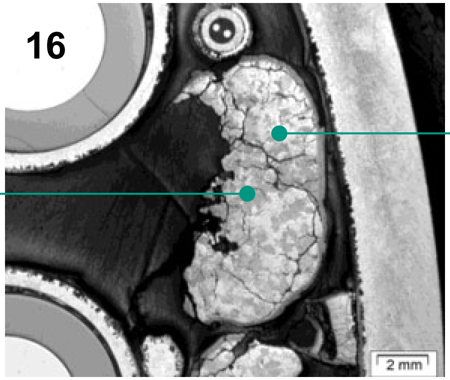

grey and light melt regions

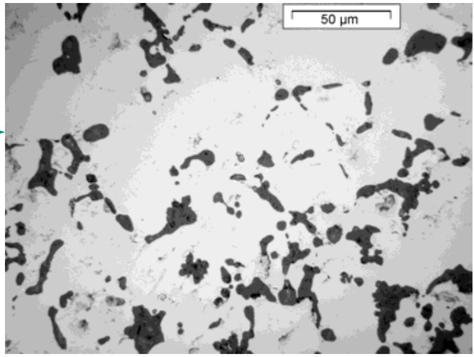

light non porous region;
precipitates 10% → **C_O = 8 wt%**

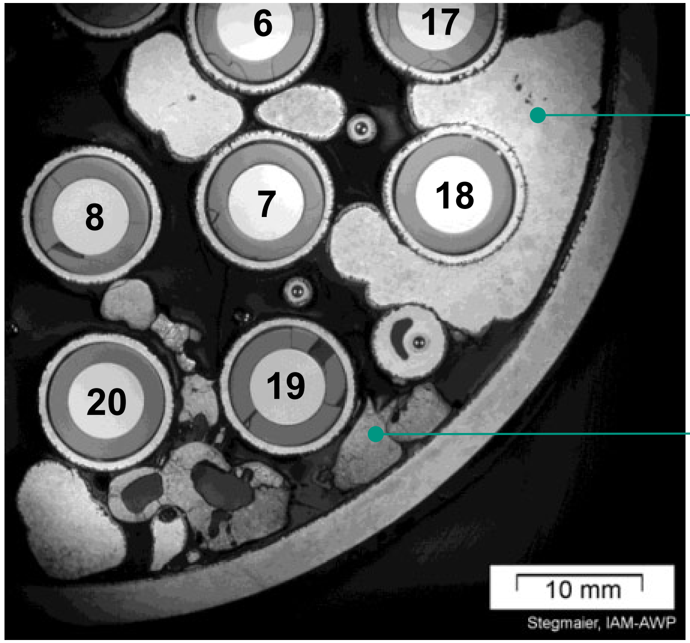

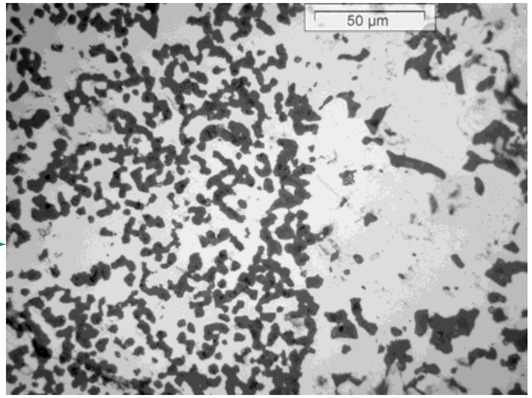

precipitates part 20% → **C_O = 10 wt%** [http://bibliothek.fzk.de/zb/berichte/FZKA6383.pdf]

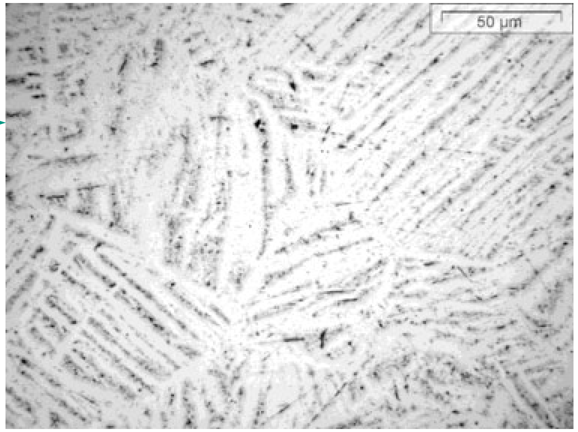

Widmanstätten pattern
of frozen metallic melt

Frozen melt at elevation 450 mm: mostly oxidised melt

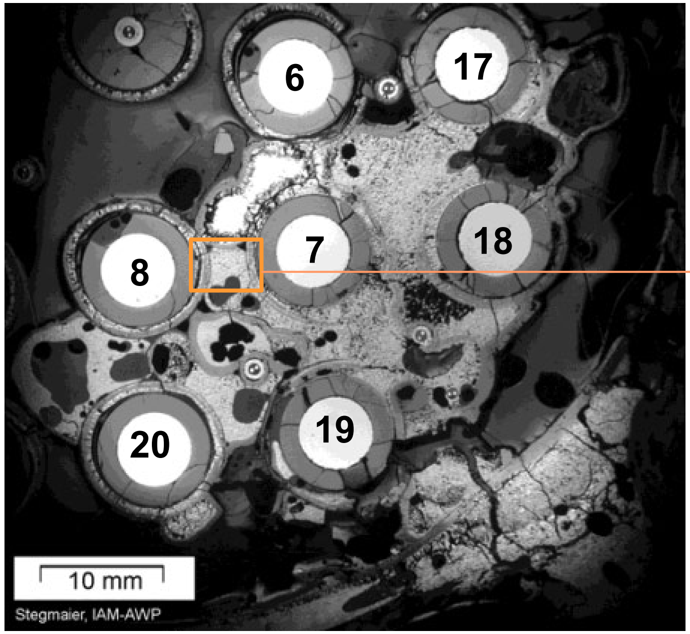

Stegmaier, IAM-AWP

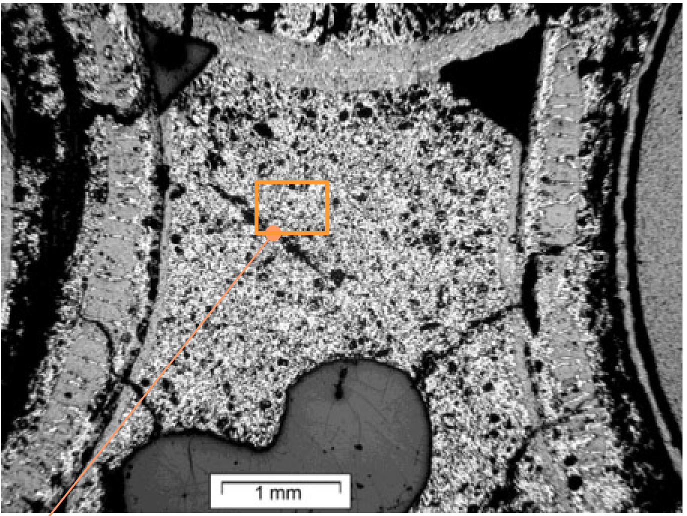

molten pool between two rods: oxidation at melt periphery and ceramic precipitates inside melt

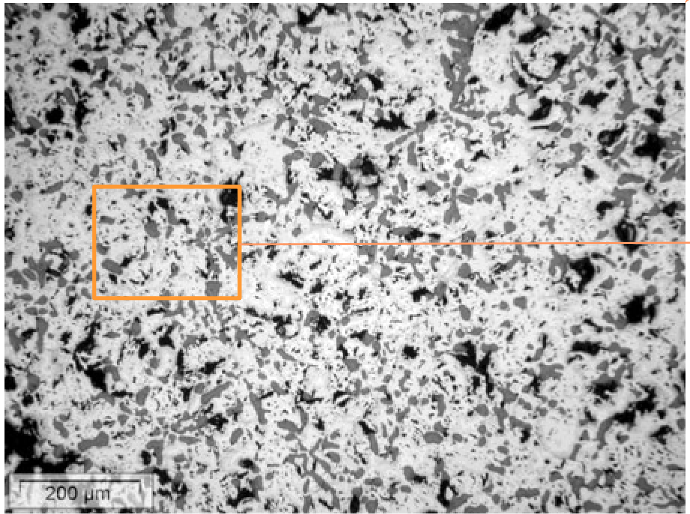

homogeneous distribution of ceramic precipitates in the melt

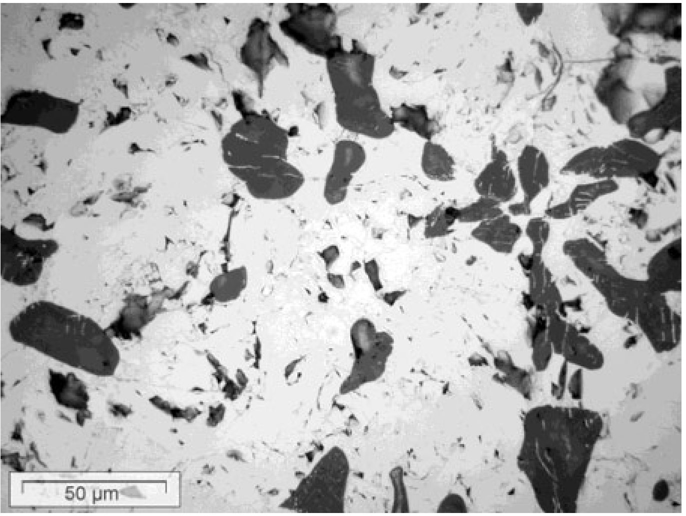

precipitates part 28% → C_O = 11.5 wt%

SUMMARY

- Three typical features of QUENCH-16: moderate pre-oxidation to 135 µm of oxide layer (instead 500 µm for QUENCH-10), a long period of oxygen starvation during the air ingress phase (800 s instead 80 s for QUENCH-10), and reflood initiation at temperatures significantly below the melting point of the cladding (1700 K instead of 2200 K for QUENCH-10).

- A partial consumption of nitrogen during the oxygen starvation, accompanied by acceleration of the temperature increase at mid bundle elevations, caused the formation of *porous* zirconium nitrides inside the oxide layer at bundle elevations between 350 and 850 mm.

- Immediate temperature escalations to 2420 K after reflood initiation were caused by massive steam penetration through the *porous* oxide/nitride scales and intensive reaction with nitrides and especially with metallic cladding. The cooling phase to the final quench lasted ca. 500 s after achievement of peak temperature.

- 24 g nitrogen from 29 g, consumed during oxygen starvation period, were released during the quench phase. This quantity of released nitrogen corresponds to **7 g** hydrogen developed during re-oxidation of nitrides.

SUMMARY (cont.)

- Metal part of different rods at elevations between 450 and 950 mm was melted during reflood. Practically all melt formed at 650 mm was released into the space between rods and relocated to the lower positions. Melt at other elevations was partially kept between rods and pellets with formation of internal oxide layer adjacent to pellet.

- Relocated melt was frozen between rods at elevations between 300 and 500 mm. Image analysis of the Zr-O melt, frozen in these pools and inside rods, allows estimating the <u>hydrogen release due to melt oxidation to **25 g**</u>.

- <u>The main part of hydrogen</u> production during reflood (<u>**96 g**</u>) was released due to <u>secondary cladding oxidation</u> by steam penetrated through the porous re-oxidized nitrides.

- The total hydrogen production during QUENCH-16 was higher compared to QUENCH-10, i.e., 144 g (QUENCH-10: 53 g), 128 g of which were released during reflood (QUENCH-10: 5 g).

Acknowledgement

The QUENCH-16 test was performed in framework of the LACOMECO program at KIT with financial support from the HGF Program NUKLEAR and the European Commission.

The authors would like to thank Mr. Große, Mr. J. Moch, Mr. Rössger, Mrs. J. Laier, Mrs. Stegmaier and Mrs. U. Peters for intensive work during the test preparation and post-test investigations.

Thank you for your attention

http://www.iam.kit.edu/wpt/english/471.php/
http://quench.forschung.kit.edu/